

The augmented lipid productivity in an emerging oleaginous model alga *Coccomyxa subellipsoidea* by nitrogen manipulation strategy

Chao Wang¹ · Zhenyao Wang¹ · Fei Luo¹ · Yuqin Li¹

Received: 19 May 2017 / Accepted: 21 July 2017 / Published online: 27 July 2017
© Springer Science+Business Media B.V. 2017

Abstract The lipid productivity controlled by both of biomass and lipid content was really crucial for economic-feasibility of microalgae-based biofuels production. This study attempted at augmenting lipid productivity in an emerging oleaginous model alga *Coccomyxa subellipsoidea* by different nitrogen manipulation including one-stage continuous N-sufficiency (OCNS), N-deprivation (OCND), N-limitation (OCNL), and also two-stage batch N-starvation (TBNS). Amongst four tested nitrogen manipulation strategies, OCNS performed remarkable promoting effect on cell metabolic growth and the maximum biomass was achieved by 7.39 g/L. Whereas TBNS regime induced the highest lipid content (over 50.5%). Only OCNL treatment augmented the lipid productivity by 232.37 mg/L/day, representing 1.25-fold more than TBNS and even as much as 5.06-fold more than that of OCND strategy. OCNL also strengthened the proportions of saturated (C16:0 and C18:0) and monounsaturated fatty acid (C18:1) which were inclined to high-quality biofuels-making. This might be due to that most part of energy and metabolic flux (e.g. acetyl-CoA) derived from TCA cycle and glycolysis flowed into fatty acids biosynthesis pathway (especially C18:1) response to OCNL manipulation. This study represented a pioneering work of utilizing OCNL for lipids production by *C. subellipsoidea* and clearly implied that OCNL might be a feasible way for algal lipid production on a commercial scale and also promoted the potential of *C. subellipsoidea* as an ideal biodiesel feedstock.

Keywords *Coccomyxa subellipsoidea* · Nitrogen manipulation · Lipid · Fatty acids · Metabolites

Introduction

Microalgae displayed ecological and commercial importance as the base of the food chain and producers of oxygen and natural source of valuable compounds such as fatty acids, carotenoids, and toxins. Microalgae have also been suggested as a competitive alternative feedstock for biofuels production due to depleting resources and the environmental problems associated with fossil fuel consumption (Guccione et al. 2014). However, microalgae-based biofuels were not economically-feasible due to the low lipid productivity of microalgae. To tackle the commercialization of algal biofuels, many endeavors have been made to improve strain performances (Yao et al. 2014), culture systems (Chen et al. 2011), and also the downstream harvesting/extraction technologies (Wan et al. 2015). Amongst all attempts, microalgae cultivation was generally regarded as vitally-important and technically-difficult procedure since the growth mediums and conditions would directly affect the quality and quantity of lipids as well as the downstream biodiesel production (Arumugam et al. 2013).

It has been well-documented that the versatile chemical or physical growth conditions such as nutrition-deprivation, high-salinity, and high-irradiance could effectively trigger lipid accumulation in microalgae cells. Nitrogen-deficiency might be the most preferable strategy to induce lipid biosynthesis due to its high-efficiency and universal-applicability amongst microalgae. However, the high lipid produced under N-deficiency usually had detrimental effects on cell growth and lead to biomass losses consequently lower overall lipid productivity (Benavente et al.

✉ Yuqin Li
yuqinli2004@126.com

¹ Biological Engineering Department, School of Chemical Engineering, Xiangtan University, Xiangtan 411105, People's Republic of China

2016). Some studies had been undertaken to enhance the overall lipid productivity under N-deficiency condition with modulation and/or supplementation of other nutrients for synergistic effects. For instance, a traditional two-stage batch N-starvation regime that was to maximize cell biomass by inceptive nutrient-sufficient medium followed lipid accumulation by N-deficiency was proposed by many researchers. Reflecting upon the vast majority of scientific publications on algal lipid accumulation, this strategy positively achieve the high lipid productivity by many microalgal species like *Chlorella*, *Scenedesmus* and *Desmodesmus* species (Peccia et al. 2013; Pancha et al. 2014; Rios et al. 2015). However, such two-stage nitrogen manipulation process usually involved higher capital cost, additional harvesting and medium requirement. Recent evidence showed that one-stage continuous N-limitation strategy which belongs to the category of N-deficiency could offer important advantages in terms of downtime reduction and operation flexibility under outdoor condition (Klok et al. 2014). The flexibility of N-limitation strategy has been already demonstrated for lipid production in *Chlorella vulgaris* (Liu et al. 2016). However, the strategy and magnitude of N-deficiency required to stimulate lipid formation was distinctively different among microalga species. Han et al. (2013) reported a high lipid productivity of 115 mg/L/day by *C. pyrenoidosa* treated with two-stage batch N-starvation strategy. Whereas *Nannochloropsis* had good performance by a maximum lipid productivity of 29.44 mg/L/day under continuous N-limitation condition (Meng et al. 2015). These discrepancies might be caused by the tremendous biodiversity of microalgae, e.g., nitrophilous versus oligonitrophilic species. Therefore, the current nitrogen manipulation strategies needed to be further explored whether it is commonly applicable for other emerging oleaginous model alga species.

Trebouxiophyceae *Coccomyxa subellipsoidea* C-169 was a type of small elongated non-motile unicellular green alga and was from algal peat in polar Antarctica. *C. subellipsoidea* has been gradually served as a new model resource for high-quality biofuels on account of (1) a relatively high growth rate and lipid content; (2) the lack of a rigid cell wall to simplify lipid extraction and genetic manipulation; (3) psychrotolerant characteristics makes mass outdoor cultivation possible by decreasing contamination; and also (4) known whole genome sequences. Currently, many studies concerned physiological-biochemical traits of this polar microalga response to cold adaptation and heavy metal ions (Blanc et al. 2012; Kováčik et al. 2015), few involved deeply the lipid accumulation in *C. subellipsoidea* under some infaust environmental conditions. It was worth noting that that N-deficiency triggered early synthesis of starch followed by lipid accumulation in *C. subellipsoidea* by the report of Msanne et al. (2012).

Allen et al. (2015) also found an increment in lipid content in *C. subellipsoidea* through nitrogen stress. These preliminary studies were encouraging and demonstrated the lipid biosynthesis of *C. subellipsoidea* could be effectively regulated by exoteric chemical or physical environmental factors.

The scenario in this study was to probe the possibilities of using nitrogen manipulation strategies (one-stage continuous N-deficiency, N-sufficiency, N-limitation, and two-stage batch N-starvation) to augment lipid productivity by *C. subellipsoidea*. The biomass, lipid content, and also fatty acid profiles would be employed to elucidate the most favorable nitrogen manipulation strategy as well as identify biochemical characteristics that resulted in maximizing lipid productivity of *C. subellipsoidea*. Metabonomics was further used to capture the comprehensive metabolite profiles related to lipid biosynthesis and further understand the interdependence of these anabolic and catabolic metabolites under the optimal nitrogen manipulation. The findings of this study was also critical to promote the practical application of *C. subellipsoidea* in biofuels industry.

Materials and methods

Materials and chemicals

Coccomyxa subellipsoidea C-169 (strain # NIES 2166) was purchased from the Microbial Culture Collection, National Institute for Environmental Studies, Japan. All chemicals were of the highest purity available.

Microalgae cultivation

Algal seed culture was initiated by a single colony taken from the stock agar plate into a 250 mL Erlenmeyer flask with 100 mL of the improved liquid Basal medium (Shi et al. 1997), which contained 1 g $\text{MgSO}_4 \cdot 7\text{H}_2\text{O}$, 1.25 g KH_2PO_4 , 0.5 g EDTA, 114.2 mg boron, 111.0 mg CaCl_2 , 49.8 mg $\text{FeSO}_4 \cdot 7\text{H}_2\text{O}$, 38.2 mg $\text{ZnSO}_4 \cdot 7\text{H}_2\text{O}$, 15.7 mg $\text{CuSO}_4 \cdot 5\text{H}_2\text{O}$, 14.4 mg $\text{MnCl}_2 \cdot 4\text{H}_2\text{O}$, 11.92 mg $\text{Na}_2\text{MoO}_4 \cdot 2\text{H}_2\text{O}$, 4.9 mg $\text{CoNO}_3 \cdot 6\text{H}_2\text{O}$, 1.25 g KNO_3 , and 10.0 g glucose in 1 L of distilled water (pH adjusted prior to autoclaving to 6.1). Erlenmeyer flask was equipped with self-made cotton plug functioned as interchange of air or oxygen supply as well as contamination control. The algal seed was then pre-cultured for 192 h at constant 28 ± 1 °C and T8 LED fluorescent lamp (three light tubes) as light source to provide light irradiance of $50 \mu\text{mol}/\text{m}^2/\text{s}$. The lamp specifications were constituted by Light intensity: 1000 ± 50 lx Rated power: 10 watts; Wave ranges: 420–740 nm; Life time: 2500–3125 day; Light color temperature: 6000 K; Usage time: 20,000–25,000 h; Reflector

specification: 0.02–0.5. Subsequently, the pre-cultured seed liquid was inoculated and cultured in different nitrogen manipulation medium to evaluate the lipid productivity of *C. subellipsoidea*. The different nitrogen manipulation strategies in detail was as follows:

1. One-stage continuous nitrogen-limitation strategy: Firstly, 1 mL of the pre-cultured seed liquid (approximate 0.1 g/L) was taken as inoculum into 250 mL Erlenmeyer flask loaded with 100 mL of sterilized liquid media, which contained the same components with Basal medium for liquid seed cultivation except for 0.5, 0.75, and 1.0 g/L KNO_3 (N-limitation concentrations) instead of 1.25 g/L KNO_3 (N concentration of standard Basal). Subsequently, all cultures in Erlenmeyer flask were induced on a reciprocating shaker (160 rpm/min) at 28 ± 1 °C with $70 \mu\text{mol}/\text{m}^2/\text{s}$ of light intensity by T8 LED fluorescent lamp. 0.0 g/L (one-stage continuous nitrogen-deficiency) and 3.0 g/L KNO_3 (one-stage continuous nitrogen-sufficiency) in Basal media were set as control cultures. It was worth noting that all the concentrations of KNO_3 were added into Basal medium from the beginning of cultivation until biomass harvest.
2. Two-stage batch nitrogen-starvation strategy: 1 mL of the pre-cultured seed liquid (approximate 0.1 g/L) was inoculated into 100 mL of sterilized Basal media containing the same components as Basal medium used for seed liquid and cultured on a reciprocating shaker (160 rpm/min) at 28 °C with constant light intensity of $70 \mu\text{mol}/\text{m}^2/\text{s}$ (First-stage); In Second-stage, the algal cells in stationary phase in First-stage were harvested by removal of the residual media and washed with sterile deionized water. And then the algal paste cells were re-suspended into 100 mL sterilized Basal media without supplementation of KNO_3 . The cultivation was performed on a reciprocating shaker (160 rpm/min) at 28 °C with constant light intensity of $70 \mu\text{mol}/\text{m}^2/\text{s}$.

All cultures consist of one-stage continuous nitrogen-limitation, two-stage batch nitrogen-deficiency, and control groups were conducted in three biological duplicates. The biomass and the lipid content were determined at 12–24 h interval.

Analytical methods

Biomass yield measurement

Algal cells in 3–5 mL culture were harvested by centrifugation at 8000 rpm/min for 20 min and the algal pellets were washed several times with distilled water until the clarified washing liquid. The wet cells were subsequently

lyophilized into algal powder to determine the biomass yield by the cell dry weight method.

Total lipid content

Up to 20 mg of lyophilized algal powder was accurately blended with 0.5 mL of distilled water and disrupted using a microwave oven at a high temperature (about 100 °C and 2450 MHz) for 5 min. Chloroform/methanol (2:1, V/V) was then introduced into the mixtures and tempestuously shaken by hybrid oscillator for 30 min. The extraction procedure was repeated three to five times. All the chloroform phases were collected by centrifugation at 8000 rpm/min for 10 min and evaporated by nitrogen flow. The lipid content was calculated by the difference between the two weights and was expressed as % of dry cell weight.

Fatty acids analysis

The algal cells used for fatty acid profiles analysis were harvested by centrifugation at 8,000 rpm/min for 30 min and the algal pellets were lyophilized by a freeze dryer (ND-10N, Henan, China). Five milligrams of freeze-dried powdered *C. subellipsoidea* sample was weighed and saponification at 85 °C in a thermostated water bath for 1 h by adding NaOH– CH_3OH solution. The boron trifluoride–methanol (1:2, V/V) was then added to the saponified solutions and vortexed for 30 min. 1 mL of hexane was used to extract the resulting fatty acid methyl esters (FAMES) for 1 h at room temperature. Subsequently, 10 μL of 100 $\mu\text{g}/\text{mL}$ 2-chloronaphthalene (Tokyo Chemical Industry, Tokyo, Japan) in hexane was added to 90 μL of the upper phase before gas chromatography–mass spectrometry (GC–MS) analysis. Samples were analyzed by using a gas chromatograph (model 7890A, Agilent Technologies) equipped with a mass-selective detector (model 5975C, Agilent Technologies), an autosampler (7683B series, Agilent Technologies), a split/splitless injector, an injection module, and ChemStation software. A capillary column (Agilent DB-23; 30 m \times 0.25 mm \times 0.25 μm) was used. The carrier gas was helium at a flow rate of 1.00 mL/min; the split ratio was 50:1; the injection volume was 1.0 μL ; the solvent delay time was 2 min; the injection temperature was 250 °C; and the flame ionization detector (FID) temperature was 270 °C. The initial oven temperature was set at 130 °C for 1 min, increased to 200 °C at a rate of 5 °C/min, and then held for 7 min. The mass range was 40–400 Da and data were obtained in full scan mode. Fatty acids were identified by autoscan and direct comparison of their mass spectral pattern, and the retention index was determined with the NIST08.LIB mass spectral database.

Global metabolomics analysis

50 mg of each freeze-dried sample was separately transferred into microfuge tubes (Eppendorf, Hamburg, Germany) and then the distilled water and methanol (V/V, 1:1) was introduced to the lyophilized samples. The mixtures were vortexed for 5 min and sonicated by ultrasonic broken instrument (Sonics VCX130, USA) for approximate 1 min in ice-water bath. The supernatant was collected separately from each sample by centrifugation (13,000 rpm/min) for 15 min at 4 °C. Totally 700 µL of supernatant for each sample was evaporated with nitrogen gas and was then used for lyophilization at -80 °C. 600 µL of each sample was re-dissolved in purified water and vortexed for 1 min. All the samples were passed through syringe filters (1.7 cm²) with a 0.45 µm pore-size PTFE membrane (Minisart SRP 15, Sartorius, Germany). Subsequently, 50 µL of trimethylsilylpropanesulfonic acid was added into all filtrate and vortexed for 1 min. The supernatant was collected by centrifugation (13,000 rpm/min) for 2 min at 4 °C and then used for acquisition NMR spectra by using a Bruker AV III 600 MHz spectrometer equipped with an inverse cryoprobe at 25 °C through a total of 32 scans over a period of 3.5 min. The first increment of a 2D-¹H, ¹H-NOESY pulse sequence was used for the acquisition of ¹H-NMR data and for suppressing the solvent signal. Spectral analysis was done using Chenomx NMR suite software version 8.1. (Chenomx Inc., Edmonton, Canada). All the spectra were referenced to the internal standard, DSS and analyzed by experienced analysts against Chenomx Compound Library.

Results

Effect of different nitrogen manipulation on biomass and lipid content of *C. subellipsoidea*

The biomass and lipid content of *C. subellipsoidea* subjected to different nitrogen manipulation including two-stage batch nitrogen-starvation (TBNS), one-stage continuous nitrogen-limitation (OCNL), nitrogen-deprivation (OCND) and nitrogen-sufficiency (OCNS) were illustrated in Fig. 1. As schematically depicted in Fig. 1a (TBNS strategy), the cell biomass was gradually increased in First-Stage and achieved the maximal value by 4.52 g/L at 168 h. And then the algal cells growth tended towards stability within 168–192 h. Subsequently, the algal cells from first-stage at 192 h were collected and re-suspended into N-starvation medium for the following second-stage cultivation. It could be seen that the biomass showed a slight increase from 4.52 to 4.68 g/L within initial 12 h of Second-Stage cultivation and then decreased from 4.68 to 3.38 g/L in the range of 12–72 h of N-starvation induction. Although

nutrition-sufficiency favored the cell growth, it was useless for conspicuous lipid accumulation in algal cells. As observed in first-stage of TBNS, the lipid content was only 11.12–18.13% of dry cell biomass from incipient inoculation 0–192 h (Fig. 1a). In contrast, the lipid content was dramatically increased from 19.5 to 50.5% and then slightly decreased from 50.5 to 48.8% within 36 h under complete N-starvation condition (second-stage). This phenomenon has been reported by Allen et al. (2015), where nitrogen stress (i.e. N-starvation) involved significant lipid accumulation in *C. subellipsoidea*.

OCNL belonging to the category of N-deficiency was also employed to probe effects on biomass and lipid content of *C. subellipsoidea*, OCND and OCNS were set as control groups. As indicated in Fig. 1b, all the biomass showed similar trend of first increase and then decrease during the whole cultivation process. Actually, N-sufficiency was treated as one of the most prominent contribution for the biomass accumulation, but the relatively superfluous N would disturb the normal catabolism activity thus limiting lipid biosynthesis. This exactly catered to the results of this study where the maximal biomass was achieved by 7.69 g/L under OCNS treatment (control, 3.0 g/L KNO₃). Whereas the lipid content maintained a relatively stable low level ranging from 11.12 to 16.51% (Fig. 1c). In contrast, the high lipid produced under N-deficiency usually had detrimental effects on cell growth. As shown in OCND group (control, 0 g/L KNO₃), the maximal biomass (1.95 g/L) was only a quarter of the maximal biomass of OCNS (Fig. 1b). And also a slight increase from 11.12 to 22.34% was observed in OCND-treated cells. Actually, N-deficiency herein was quite different from N-deficiency in TBNS, in which cells have not experienced nutritional cultivation and were not be provided enough exogenous energy for lipid synthesis consequently resulted in a low level increase. Amongst all OCNL experimental groups, OCNL-1.0 g/L KNO₃ performed the most remarkable promoting effect on cell growth and the maximum biomass was achieved by 5.49 g/L at 192 h. OCNL-0.5 g/L KNO₃ and OCNL-0.75 g/L KNO₃ strategies had similar stimulation effects on *C. subellipsoidea* growth and the maximum biomass was 3.75 and 4.28 g/L, respectively. Although the biomasses of OCNL groups were less than that of OCNS group, the maximal biomass of this strategy representing 2.05- to 2.69-fold more than that of OCND group (Fig. 1b; Table 1). These results indicated that the cells growth rate (accumulation of biomass) of *C. subellipsoidea* greatly depended on nitrogen availability in medium. Apart from the biomass parameter, another pivotal point affecting biodiesel refinery is the lipid content. Different N-limitation manipulations caused distinctly different lipid accumulation in *C. subellipsoidea*. When algal cells were fed with OCNL-0.5 g/L KNO₃, the lipid content showed dramatic

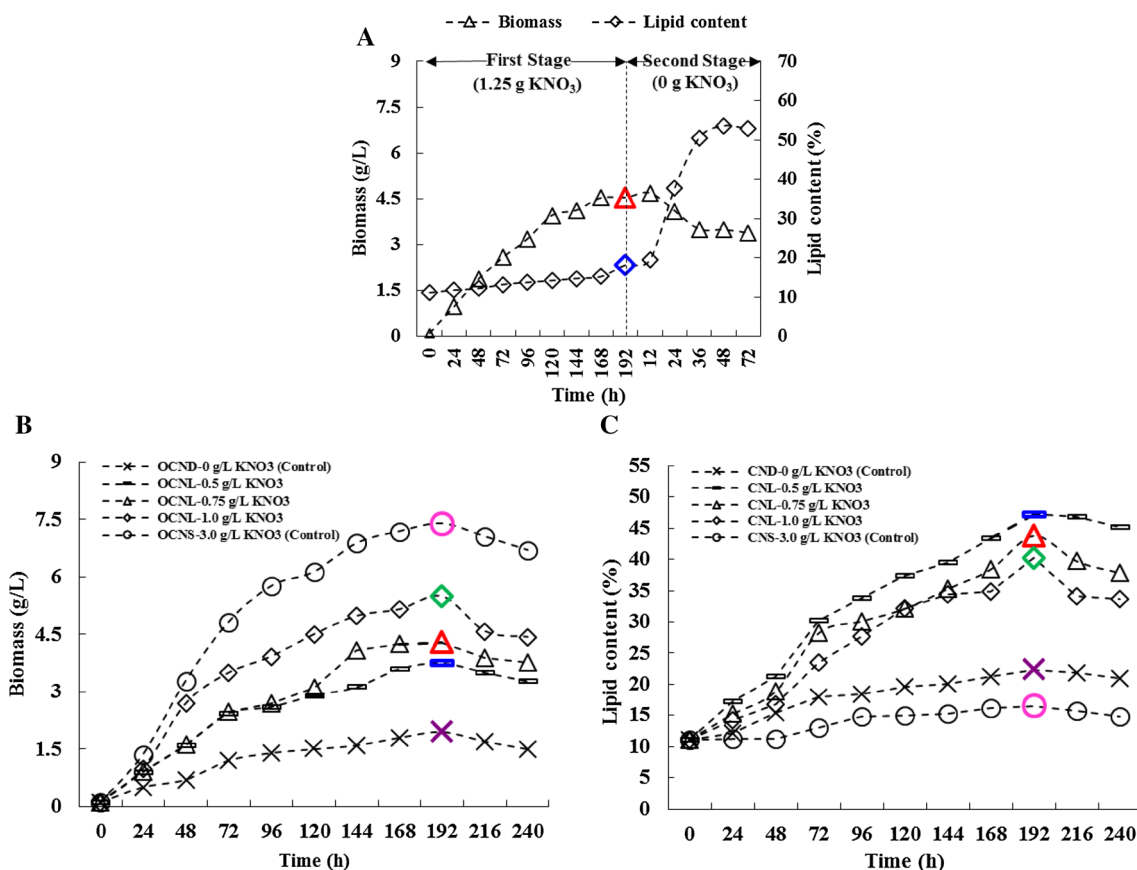


Fig. 1 Effect of different nitrogen manipulation strategies on biomass and lipid content of *C. subellipsoidea*. **a** Effects of two-stage batch nitrogen-starvation (TBNS) on biomass and lipid content of *C. subellipsoidea*. TBNS strategy was performed by two-stage cultivation: the algal cells were cultured with nutrition-sufficiency Basal medium (1.25 g/L KNO₃) to obtain favorable biomass in first stage; the algal cells in first-stage were collected and re-suspended into fresh nitrogen-starvation Basal medium (0.0 g/L instead of 1.25 g/L KNO₃) to

induce lipid accumulation in second-stage. **b** and **c** Effects of one-stage continuous nitrogen-limitation (OCNL) on biomass and lipid content of *C. subellipsoidea*. The algal cells were inoculated into nitrogen-limitation Basal medium supplied with 0.5, 0.75, 1.0 g/L of KNO₃. One-stage continuous nitrogen-deprivation (OCND, 0.0 g/L KNO₃) and continuous nitrogen-sufficiency (OCNS, 3.0 g/L KNO₃) were set as control groups. Data were shown as mean values of three independent biological replicates (n=3)

Table 1 Comparisons of different nitrogen manipulation for biomass and lipid production of *Coccomyxa subellipsoidea*

Biological indicators	TBNS	OCNL			OCNS (control)	OCND (control)
		0.5 g/L KNO ₃	0.75 g/L KNO ₃	1.0 g/L KNO ₃		
	First-stage (1.25 g/L KNO ₃)					
	Second-stage (0.0 g/L KNO ₃)					
Biomass (g/L)	3.5	3.75	4.28	5.49	7.39	1.95
Lipid content (%)	50.5	47.21	43.81	40.21	16.51	22.34
Total lipid productivity (mg/L/day)	186.05	186.35	197.38	232.37	128.43	45.85

The total lipid productivity was calculated when the biomass and lipid content reached its highest value. TBNS, OCNL, OCND, OCNS were abbreviations of two-stage batch nitrogen-starvation, one-stage continuous nitrogen-limitation, one-stage continuous nitrogen-deprivation and one-stage continuous nitrogen-sufficiency, respectively

increase with favorable content was 47.21% at 192 h, which represented 2.22- to 2.70-fold higher than that of OCND and OCNS strategies. Even though the performances of

using OCNL-0.75 g/L and OCNL-1.0 g/L KNO₃ strategies in aspect of stimulating lipid accumulation were less better than OCNL-0.5 g/L KNO₃, the relatively high lipid content

of 40.81 and 35.21% were also achieved at 192 h, respectively. These results strongly implied that N-limitation concentrations has a positive co-relation with the intracellular lipid content.

Actually, the lipid productivity controlled by both of biomass and lipid content was really crucial for economic-feasibility of microalgae-based biofuels production. The lipid productivity of *C. subellipsoidea* by different nitrogen manipulation were listed in Table 1. As shown in Table 1, all OCNL strategies performed better than TBNS and control groups in terms of achieving the high lipid productivity (Table 1). Particularly, OCNL-1.0 g/L KNO₃ showed the greatest superiority with the maximal lipid productivity was 232.37 mg/L/day, representing 1.25-fold and 1.81-fold more than TBNS and OCNS and even as much as 5.06-fold

more than that of OCND strategy (Table 1). Based on the elaborations, OCNL might be a feasible way for algal lipid productivity on a commercial scale and deserved further exploration.

Fatty acid profiles of *C. subellipsoidea* cells treated with different nitrogen manipulation

The fatty acid profiles including carbon chain length and unsaturation degree of *C. subellipsoidea* cells treated with different nitrogen manipulation (i.e. TBNS, OCNL, OCNS, and OCND) were summarized in Table 2. The results demonstrated that no distinct difference in fatty acid profiles was observed in all nitrogen manipulation cultures, being mainly composed of C16 and C18 fatty

Table 2 Fatty acid compositions of *Coccomyxa subellipsoidea* cells treated with different nitrogen manipulation

CX:Y ^a	Fatty acid components	RT	Relative content (%)					
			OCND (control)	OCNS (control)	TBNS	OCNL-0.5 g/L KNO ₃	OCNL-0.75 g/L KNO ₃	OCNL-0.1 g/L KNO ₃
C16:0	Palmitic acid	19.34	14.33 ± 1.13	16.74 ± 1.06	15.69 ± 1.13	17.39 ± 1.12	17.22 ± 1.16	18.88 ± 1.11
C18:0	Octadecanoic acid	24.71	2.87 ± 0.03	2.43 ± 0.02	2.76 ± 0.01	2.32 ± 0.03	1.71 ± 0.02	1.96 ± 0.01
C18:1	Oleic acid	25.30	14.09 ± 1.22	16.73 ± 1.22	16.03 ± 1.20	32.24 ± 1.02	34.11 ± 1.22	42.13 ± 1.02
C16:2	Hexadecadienoic acid	20.74	4.22 ± 0.07	3.89 ± 0.04	4.05 ± 0.03	3.19 ± 0.05	3.16 ± 0.03	2.64 ± 0.06
C16:3	Hexadecatrienoic acid	22.45	3.57 ± 0.02	2.82 ± 0.06	3.13 ± 0.05	2.58 ± 0.02	2.33 ± 0.01	0.94 ± 0.04
C18:2	Linoleic acid	26.88	15.44 ± 0.11	16.06 ± 0.20	15.88 ± 0.21	16.19 ± 0.23	16.62 ± 0.21	17.06 ± 0.35
C18:3	Linolenic acid	29.43	13.78 ± 0.03	12.17 ± 0.05	12.88 ± 0.03	10.77 ± 0.03	10.90 ± 0.04	7.44 ± 0.06
	ΣSFAs		17.20 ± 0.13	19.17 ± 0.11	18.45 ± 0.13	19.71 ± 0.13	18.93 ± 0.18	20.84 ± 0.15
	ΣMUFAs		14.09 ± 1.22	16.73 ± 1.11	16.03 ± 1.21	32.24 ± 1.22	34.11 ± 1.20	42.13 ± 1.09
	ΣSFAs+MUFAs		31.29 ± 2.20	35.90 ± 1.89	34.48 ± 1.78	51.95 ± 3.21	53.04 ± 3.28	62.97 ± 3.47
	ΣPUFAs		37.01 ± 0.03	34.94 ± 0.03	35.94 ± 0.06	32.73 ± 0.03	33.01 ± 0.09	28.08 ± 0.07
	ΣTFA		68.30 ± 1.02	70.84 ± 1.11	70.42 ± 1.15	84.68 ± 1.32	86.05 ± 1.12	91.05 ± 1.08
	Unidentified		31.70 ± 0.22	29.16 ± 0.44	29.58 ± 0.21	15.32 ± 0.33	13.95 ± 0.14	8.95 ± 0.11

The variations of fatty acids in OCNL-1.0 g/L KNO₃-treated *C. subellipsoidea* cells at different growth stages

CX:Y ^a	Fatty acid components	Relative content (%)		
		144 h	192 h	216 h
C16:0	Palmitic acid	19.35 ± 1.02	18.88 ± 1.11	16.76 ± 0.95
C18:0	Octadecanoic acid	1.33 ± 0.01	1.96 ± 0.01	1.85 ± 0.02
C18:1	Oleic acid	24.28 ± 0.62	42.13 ± 1.02	31.12 ± 1.02
C16:2	Hexadecadienoic acid	5.06 ± 0.02	2.64 ± 0.06	1.18 ± 0.02
C16:3	Hexadecatrienoic acid	2.00 ± 0.01	0.94 ± 0.04	0.62 ± 0.01
C18:2	Linoleic acid	10.54 ± 0.28	17.06 ± 0.35	16.84 ± 0.11
C18:3	Linolenic acid	6.48 ± 0.06	7.44 ± 0.06	7.32 ± 0.21

^aThe notation in the form of CX:Y, where X is the carbon number of the fatty acid chain and Y is the number of double bonds. TFA and RT were the abbreviations of total fatty acid and retention time. The abbreviations of various nitrogen manipulation were consistent with the footnotes of Table 1. SFAs, MUFAs, and PUFAs indicated the saturated fatty acids, monounsaturated fatty acids, and polyunsaturated fatty acids, respectively. The fatty acid compositions and contents were analyzed when the algal biomass achieved the highest lipid productivity. Data are shown as the mean ± standard deviation (SD) values for three independent biological replicates (n = 3). The attached list showed the variation of fatty acids in OCNL-1.0 g/L KNO₃-treated *C. subellipsoidea* cells at different growth stages, which would be used for "Discussion" section

acids. This was consistent with the previous reports where the similar fatty acid profiles were detected in *C. subellipsoidea* and the same genus *C. vulgaris* cells (Hultberg et al. 2014; Allen et al. 2015). These detected fatty acid compositions were also extremely similar to plant fatty acid components, which indicated the potential of *C. subellipsoidea* as an ideal biodiesel feedstock. However, as listed in Table 2, the proportion of individual fatty acid was distinctively different amongst different nitrogen manipulation strategies. The dominant FAs in OCND-treated cells (control) were palmitic acid (C16:0, 14.33%), oleic acid (C18:1, 14.09%), linoleic acid (C18:2, 15.44%), and linolenic acid (C18:3, 13.78%). And the summation of SFAs and MUFAs was present as 31.29%, which was less than the proportion of PUFAs (37.01%). In OCNS- and TBNS-treated cells, the proportions of the main C16:0, C18:1, C18:2, and C18:3 showed slight increases in comparison with OCND control, accounting for 16.74 and 15.69%, 16.73 and 16.03%, 16.06 and 15.88%, 12.17 and 12.88%, respectively. The PUFAs were reduced and the current percentages of PUFAs (35.94 and 34.94%) closed to the summation of SFA and MUFA (35.90 and 34.48%) in OCNS and TBNS. As for OCNL strategies, C16:0, C18:1, and C18:2 were significantly increased as well as C18:3 showed slight decrease in comparison with controls and TBNS. The content of C18:3 (7.44–10.90%) easily complied with the specifications established by ASTM D-6751 and EN 14214 related to biodiesel quality. It was worth noting that C18:1 showed great fluctuation by different nitrogen manipulation. It was especially rich in OCNL-0.1 g/L KNO₃ treated cells by occupying approximate 42.13% of total FAs, which was 1.24- to 2.99-fold more than that of controls, TBNS, and other OCNL strategies. In fact, algal lipids containing high oleic acid usually provide the greater stability for biodiesel production. Moreover, the summation of SFA and MUFA was higher than the PUFAs in all OCNL strategies. Especially, the percentages of SFAs and MUFAs dominated, accounting for 62.97% in OCNL-0.1 g/L KNO₃ treated cells, which was far more than the proportion of PUFA (28.08%). Correspondingly, the summation of SFAs and MUFAs (51.95% and 53.04%) in OCNL-0.5 g/L KNO₃ and OCNL-0.75 g/L KNO₃ treated cells also exceeded the total contents of PUFAs (32.73 and 33.01%), respectively. Whereas such high content of SFAs and MUFAs over PUFAs in algal cells could endow superior oxidation stability and lower viscosity properties for algae-based biodiesel (Knothe 2014). Taken together, the aforementioned results are encouraging and then again imply the great potential of OCNL strategy to produce desired FAs for sustainable biodiesel production.

Effect of nitrogen manipulation strategy on intracellular metabolites of *C. subellipsoidea*

The above elaborations (“Effect of different nitrogen manipulation on biomass and lipid content of *C. subellipsoidea*” and “Fatty acid profiles of *C. subellipsoidea* cells treated with different nitrogen manipulation”) clearly indicated the best performance with regard to augmenting lipid productivity by *C. subellipsoidea* when one-step continuous N-limitation (OCNL-0.1 g/L KNO₃) worked. In order to expand the potential applications of OCNL strategy in other algae system, NMR-based metabolomics was employed to investigate the changes of metabolites related to lipid synthesis in *C. subellipsoidea*. A total of 45 differently expressed hydro-soluble small molecules metabolites, including 22 amino acids and derivatives, six amines and ammoniums compounds, eight organic acids, seven nucleic acid components, and two others compounds were identified and quantified in OCNL-treated cells (Table 3). These 45 metabolites were classified into carbohydrate metabolism, amino acid metabolism, pyruvate and TCA metabolism, lipid metabolism, methane metabolism, urea cycle, purine metabolism, and other unknown metabolic activities. Further, multivariate statistical analysis including principal component analysis (PCA) and partial least square-discriminant analysis (PLS-DA) was performed to characterize the significant differences of metabolites in OCNL-treated cells at three time points (144, 192, and 216 h) (Fig. 2a–c). Both analysis models were well constructed with excellent fit and satisfactory predictive ability ($Q^2=0.988$, $R^2=0.957$). The unsupervised clustering method PCA was used to identify and rank major components of variance within the three data sets. As indicated in Fig. 3a, samples in different OCNL treatment time points (144, 192, and 216 h) were separated clearly on the PCA score plot. The first principal component (PC1) accounted for 74.2% of the total variance among the three experimental groups. A PCA plot of PC1 vs. PC2 (two components account for 91.0% of the variance) clearly separates the three group samples treated with OCNL. And most individual biological replicate samples (three replicates for each time point) tended to be clustered together, which demonstrated an overall good reproducibility. These results indicated that the metabolic profiles of OCNL-treated cells differ significantly at three time points. The supervised clustering PLS analysis results further supported such intriguing discrepancy (Fig. 2b). Meanwhile, principal components in the VIP maps were selected as differential signals according to variables with VIP >1. As shown in Fig. 2c, there were six metabolites with VIP value >1 in the VIP plot, including sucrose, lactate, glutamate, proline, sn-Glycero-3-phosphocholine, and valine. To further shed light on the potential relations between these metabolites

Table 3 Global metabolites in *C. subellipsoidea* cells treated with OCNL strategy

Classification ^a	Component ^b	Formula ^c	Biological function	Metabolite concentration (mg/g) ^d		
				144 h	192 h	216 h
Amines	Ethanolamine	C ₂ H ₇ NO	Lipid metabolism	1.9000 ± 0.1209	1.0780 ± 0.0124	0.493 ± 0.0116
	Methylguanidine	C ₂ H ₇ N ₃	Unknown	0.0140 ± 0.0061	0.0311 ± 0.0113	0.0365 ± 0.0147
	Trimethylamine	C ₃ H ₉ N	Methane metabolism	0.0041 ± 0.0003	0.0042 ± 0.0007	0.0039 ± 0.0002
Amino acid	Aminobutyrate	C ₄ H ₉ NO ₂	Amino acid metabolism	0.1944 ± 0.0556	ND	ND
	Aminolevulinic acid	C ₅ H ₉ NO ₃	Amino acid metabolism	0.0856 ± 0.0079	ND	ND
	Alanine	C ₃ H ₇ NO ₂	Amino acid metabolism	2.9480 ± 0.1684	1.684 ± 0.0808	1.3500 ± 0.0770
	Arginine	C ₆ H ₁₄ N ₄ O ₂	Urea Cycle	0.1559 ± 0.0045	0.1137 ± 0.0414	0.0951 ± 0.0341
	Asparagine	C ₄ H ₈ N ₂ O ₃	Amino acid metabolism	0.1946 ± 0.0194	0.1221 ± 0.0178	0.1092 ± 0.0208
	Aspartate	C ₄ H ₇ NO ₄	Amino acid metabolism	0.1436 ± 0.0129	0.1553 ± 0.0283	0.3390 ± 0.0203
	Glutamate	C ₅ H ₉ NO ₄	Amino acid metabolism	7.4740 ± 0.4968	8.4230 ± 0.6090	9.108 ± 0.0973
	Glutamine	C ₅ H ₁₀ N ₂ O ₃	Amino acid metabolism	0.0844 ± 0.0090	0.0448 ± 0.0135	0.0653 ± 0.0035
	Glycine	C ₂ H ₅ NO ₂	Amino acid metabolism	0.1086 ± 0.0210	0.1431 ± 0.0167	0.1377 ± 0.0109
	Histidine	C ₆ H ₉ N ₃ O ₂	Amino acid metabolism	0.0228 ± 0.0016	0.1352 ± 0.0144	0.1249 ± 0.0181
	Isoleucine	C ₆ H ₁₃ NO ₂	Amino acid metabolism	0.1276 ± 0.0060	0.1196 ± 0.0122	0.0513 ± 0.0047
	Leucine	C ₆ H ₁₃ NO ₂	Amino acid metabolism	0.0844 ± 0.0063	0.1114 ± 0.0122	0.1115 ± 0.0145
	Lysine	C ₆ H ₁₄ N ₂ O ₂	Amino acid metabolism	0.3749 ± 0.0446	0.3141 ± 0.0190	0.1693 ± 0.0066
	Methionine	C ₅ H ₁₁ NO ₂ S	Amino acid metabolism	0.0500 ± 0.0073	0.0487 ± 0.0048	0.0170 ± 0.0011
	Phenylalanine	C ₉ H ₁₁ NO ₂	Amino acid metabolism	0.0728 ± 0.0148	0.0365 ± 0.0028	0.0228 ± 0.0148
	Proline	C ₅ H ₉ NO ₂	Amino acid metabolism	0.1434 ± 0.0204	0.2538 ± 0.0169	0.5323 ± 0.0376
	Serine	C ₃ H ₇ NO ₃	Amino acid metabolism	0.9008 ± 0.0075	0.7310 ± 0.0349	0.6867 ± 0.0542
	Threonine	C ₄ H ₉ NO ₃	Amino acid metabolism	0.3284 ± 0.0293	0.2627 ± 0.0482	0.2426 ± 0.0166
	Tryptophan	C ₁₁ H ₁₂ N ₂ O ₂	Amino acid metabolism	0.0147 ± 0.0034	0.0315 ± 0.0030	0.0384 ± 0.0103
	Tyrosine	C ₉ H ₁₁ NO ₃	Amino acid metabolism	0.2286 ± 0.0034	0.1865 ± 0.0034	0.1775 ± 0.0177
Valine	C ₅ H ₁₁ NO ₂	Amino acid metabolism	0.3112 ± 0.0191	0.4804 ± 0.0239	0.5495 ± 0.0075	
β -Alanine	C ₃ H ₇ NO ₂	Amino acid metabolism	1.0342 ± 0.1013	0.3320 ± 0.0200	0.2121 ± 0.0253	
Ammoniums compounds	Choline	C ₅ H ₁₄ NO	Lipid metabolism	0.6800 ± 0.0011	0.5200 ± 0.0006	0.1300 ± 0.0039
	Phosphocholine	C ₅ H ₁₅ NO ₄ P	Lipid metabolism	0.1469 ± 0.0080	0.1344 ± 0.0070	0.0103 ± 0.0008
	sn-Glycero-3-p	C ₈ H ₂₁ NO ₆ P	Lipid metabolism	0.0692 ± 0.0031	0.2208 ± 0.0223	0.4211 ± 0.0064
Ketones	Acetoin	C ₄ H ₈ O ₂	Unknown	ND	ND	0.0002 ± 0.0001
Nucleic acid components	AMP	C ₁₀ H ₁₄ N ₅ O ₇ P	Purine metabolism	0.4758 ± 0.0038	0.5767 ± 0.0442	0.3728 ± 0.0191
	Inosine	C ₁₀ H ₁₂ N ₄ O ₅	Purine metabolism	0.0190 ± 0.0049	0.0199 ± 0.0064	0.0153 ± 0.0054
	NAD ⁺	C ₂₁ H ₂₈ N ₇ O ₁₄ P ₂	Energy metabolism	0.6459 ± 0.0167	0.6788 ± 0.0605	0.7021 ± 0.0248
	NADP ⁺	C ₂₁ H ₂₈ N ₇ O ₁₇ P ₃	Energy metabolism	0.0612 ± 0.0054	0.0963 ± 0.0167	0.1184 ± 0.0139
	UDP-galactose	C ₁₅ H ₂₄ N ₂ O ₁₇ P ₂	Carbohydrate metabolism	0.2944 ± 0.0079	0.2505 ± 0.0434	0.2600 ± 0.0448
	UDP-glucose	C ₁₅ H ₂₄ N ₂ O ₁₇ P ₂	Carbohydrate metabolism	0.4830 ± 0.0448	0.4111 ± 0.0587	0.40381 ± 0.0335
	UMP	C ₉ H ₁₃ N ₂ O ₉ P	Purine metabolism	0.0787 ± 0.0110	0.0461 ± 0.0052	0.0578 ± 0.0219
Organic acids	2-Oxoglutarate	C ₅ H ₆ O ₅	Pyruvate and TCA metabolism	0.1455 ± 0.0422	0.1162 ± 0.0034	0.0800 ± 0.0081
	Acetate	C ₂ H ₄ O ₂	Pyruvate and TCA metabolism	0.0740 ± 0.0027	0.0336 ± 0.0037	0.0301 ± 0.0061
	Formate	CH ₂ O ₂	Pyruvate and TCA metabolism	0.0079 ± 0.0023	0.0108 ± 0.0006	0.0102 ± 0.0017
	Fumarate	C ₄ H ₄ O ₄	Pyruvate and TCA metabolism	0.0714 ± 0.0026	0.0303 ± 0.0031	0.00519 ± 0.00024
	Lactate	C ₃ H ₆ O ₃	Pyruvate and TCA metabolism	4.150 ± 0.3069	1.224 ± 0.1094	0.6841 ± 0.0959
	Malate	C ₄ H ₆ O ₅	Pyruvate and TCA metabolism	0.5248 ± 0.0598	0.3460 ± 0.0055	0.2074 ± 0.0298

Table 3 (continued)

Classification ^a	Component ^b	Formula ^c	Biological function	Metabolite concentration (mg/g) ^d		
				144 h	192 h	216 h
	Methylmalonate	C ₄ H ₆ O ₄	Purine metabolism	ND	0.0088 ± 0.0017	0.0093 ± 0.0016
	Succinate	C ₄ H ₆ O ₄	Pyruvate and TCA metabolism	0.4096 ± 0.0486	0.2869 ± 0.0286	0.1324 ± 0.0102
Sugars	Sucrose	C ₁₂ H ₂₂ O ₁₁	Carbohydrate metabolism	40.29 ± 2.179	22.44 ± 2.295	21.55 ± 2.372

Metabolites ^aclassification and ^bidentification were based on Chemomx Database; ^cFormula of each metabolite was from CAS Registry; ^dMetabolites concentration was calculated by the following reduction formula: $C \text{ (mg/g)} = C_0 \times V_0 \times M/m$, where C_0 was the metabolite concentration in NMR data format (mmol/L), V_0 was the liquid volume of the extracted metabolites (L), M represented the molar mass of each metabolite (g/mol), and m indicated the weight of each sample (g). Extraction and analysis procedure of the metabolites were described in detail in "Analytical methods" Global metabolites analysis. The average metabolites concentration data are shown as the mean ± SD values for three independent biological replicates. *ND* indicated that the metabolite was not detected

and lipids biosynthesis, the biochemical pathway embracing most of detected metabolites, lipids, and fatty acids was mapped in Fig. 3. The information of metabolites were summarized in Table 3.

Discussion

It was widely accepted that nitrogen was one of the most fundamental and crucial ingredient in determining metabolic growth, photosynthetic rate and biochemical compositions (e.g. glycolipids, fatty acids, nucleic acids, and amino acids) of microorganisms, including microalgae (Wang et al. 2016). Furthermore, nitrogen has a positive role in generating and transforming metabolic energy in the form of ATP or NADPH, which were important driving forces for promoting the accumulation of metabolites in plants (Coruzzi and Bush 2001). Therefore, nitrogen received special attention when using unfavorable environmental factors to stimulate lipid accumulation in microalgae. One-stage continuous N-sufficiency (OCNS) or N-deficiency (OCND) might be the most ineptive nitrogen manipulation strategies used for microalgae and performed remarkable promoting effect on cell metabolic growth or lipid biosynthesis. However, the high-density cells produced under OCNS usually accompanied by the depressed lipid content consequently lower overall lipid productivity. And also OCND had detrimental effects on cell growth since N-deficiency could not satisfy the nutritional requirement to make microalgae slow down even cease cell division (Benavente et al. 2016). Therefore, some investigations had been attempted to enhance the overall lipid productivity under N-deficiency condition with modulation and/or supplementation of other nutrients for synergistic effects. A traditional two-stage batch N-starvation (TBNS) strategy was proposed to enhance the overall lipid productivity by ineptive nutrient-sufficient medium to maximize

cell biomass followed lipid accumulation by N-deficiency (Klok et al. 2014). Reflecting upon the vast majority of scientific publications on lipid accumulation, TBNS manipulation achieved the relatively high lipid productivity by many microalgae species like *Chlorella*, *Scenedesmus* and *Desmodesmus* species (Mujtaba et al. 2012; Pancha et al. 2014; Rios et al. 2015). Actually, this TBNS strategy was also available in *C. subellipsoidea*, which was supported by the lipid productivity of 186.05 mg/L/day in this study, representing 1.45- and 4.06- fold more than that of OCNS and OCND. However, such nitrogen manipulation process usually involved higher capital cost, additional harvesting and medium requirement due to discontinuous phase cultivation (Klok et al. 2014). Subsequently, one-stage continuous nitrogen-limitation (OCNL) emerged as a potential strategy by merging the positive aspects of N-deficiency (inhibiting cell growth) and nutrition-sufficiency (limiting lipid formation) to create the optimal conditions by regulating nitrogen concentration in medium for lipid productivity. Pancha et al. (2014) has reported the advantage of flexible in adjusting the N-limitation concentrations to promote the opportunities of accumulating tailor-made biomass compositions, such as protein, carbohydrate, and chlorophyll. Interestingly, in this study, OCNL-treatment further augmented lipid production of *C. subellipsoidea* with the favorable productivity was 232.37 mg/L/day, representing 1.25-fold more than the traditional TBNS strategy. These results strongly implied the potential of OCNL nitrogen manipulation strategy in augmenting lipid productivity of *C. subellipsoidea*.

Apart from the lipid productivity per unit mass of cells, the fatty acid compositions in lipids was also crucial factor if it was used for high-quality biodiesel production. Because biodiesel properties (i.e. oxidative stability, cold flow, and viscosity) were greatly dependent on the fatty acid compositions and the predominant components of high-quality biodiesel should be short-chain fatty acids

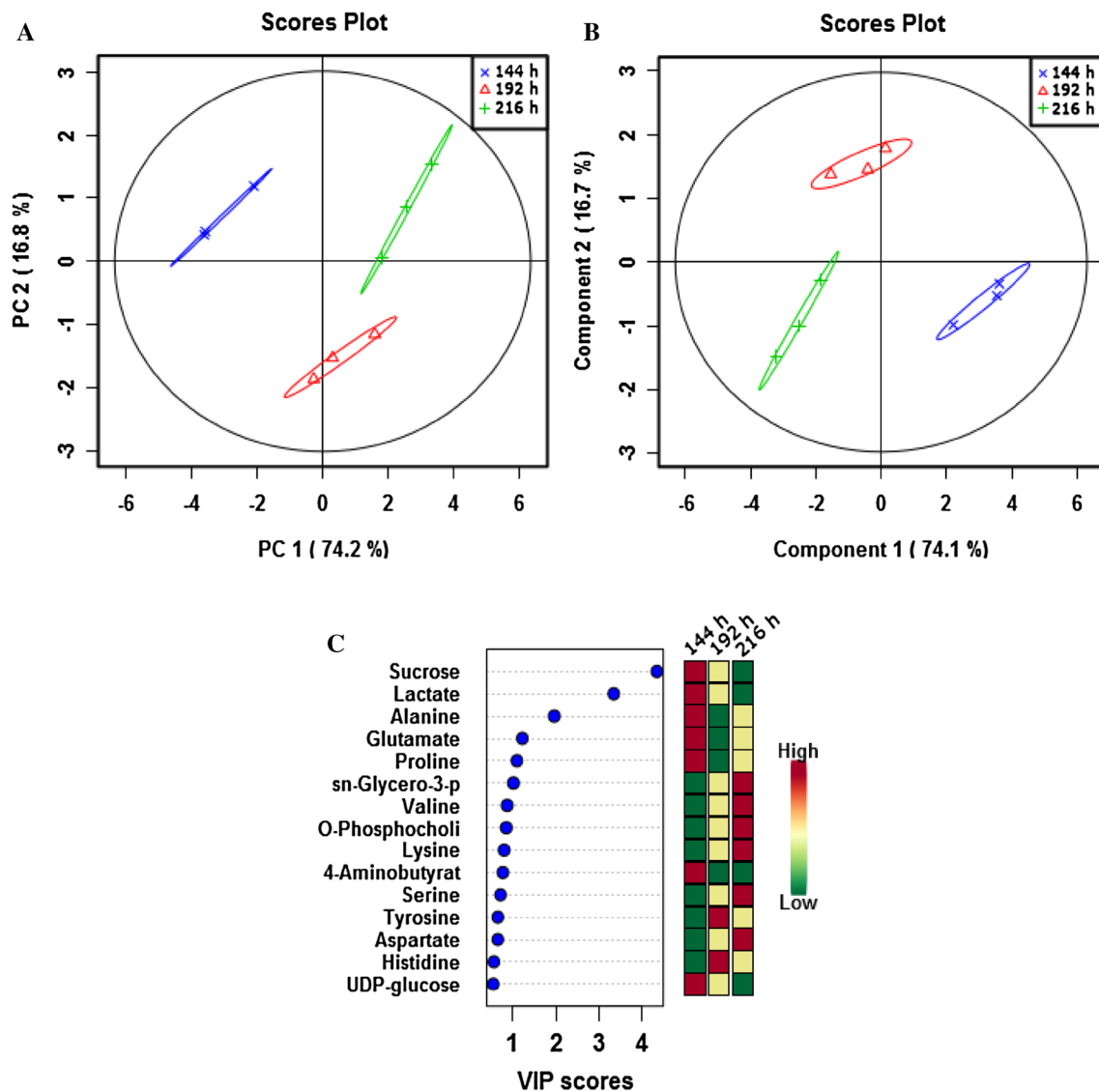


Fig. 2 PCA score plot (a), PLS-DA score plot (b), and VIP scores (c) of metabolites in *C. subellipsoidea* cells treated with OCNL at three time points (144, 192, and 216 h). Each dot represents one biological sample in PCA score plot and PLS-DA score plot while the same color and shape dots are biological replicates of each time point sample. Metabolites were listed from highest to lowest contribution

to accumulation of lipids in VIP scores figure. Variable importance in the projection of Comp.1 (VIP) ranks the contribution of each variable to lipids accumulation in OCNL-treated cells. Components were selected as significant signals according to variables with VIP >1. Abbreviations of some metabolites were adopted in order to show clearly

containing 14–18 carbon atoms (Knothe 2014; Lee et al. 2014). From this point of view biodiesel from *C. subellipsoidea* seemed to fulfil the requirements since the high percentage of C16–C18 fatty acids that constituted triacylglycerols were detected in cells. Actually, the lipids dominated by SFAs and MUFAs were favorable for oxidative stability, combustion-related properties, and cold-flow property. Although lipids rich in PUFAs had excellent performance on solidify property of biofuels, the abundant highly-unsaturated fatty acids was more susceptible to oxidation. Many previous reports indicated that a high yield of SFAs (e.g. C16:0 and C18:0) along with MUFAs (e.g. C18:1) could

endow the oxidation stability and cold-flow property for algae-based biofuels (Praveenkumar et al. 2012; Lee et al. 2014). In this study, the most valuable finding was that the summation of SFAs and MUFA (51.95–62.97%) in OCNL-treated *C. subellipsoidea* cells was just higher than the content of PUFAs (28.08–32.73%). OCNL-1.0 g/L KNO₃-treated *C. subellipsoidea* cells especially showed superiorities in achieving such percentages of fatty acids. Whereas the proportions of SFAs and MUFAs in TBNS-treated and OCNS-treated cells (control) were almost equal with individual content of PUFAs and also the SFAs and MUFAs contents in OCND-treated cells (control) was far

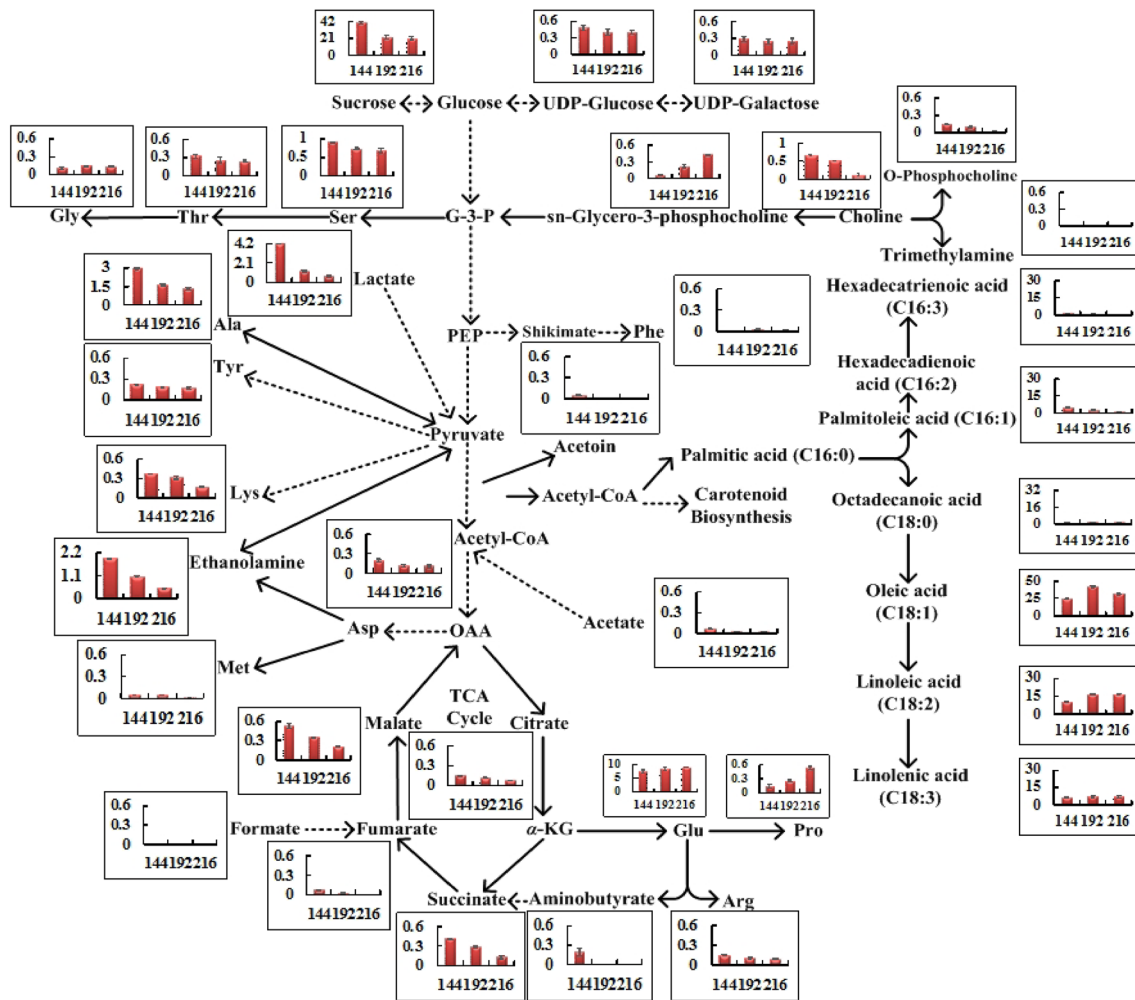


Fig. 3 Simplified scheme of lipids pathway in *C. subellipsoidea* cells with OCNL manipulation. The proposed metabolic pathways were based on KEGG database (<http://www.kegg.jp>). Diagram showing the level changes in metabolite abundance at three time points (144, 192, and 216 h) mapped onto the metabolic network. *Y*-axis value and *X*-axis represented metabolite concentration and time points.

lesser than the contents of PUFAs. Even the same species *C. subellipsoidea* worked, the summation of the SFAs and MUFAs (38.9%) in cells cultured with N-starvation was also a gap with the content of PUFAs (60.0%) (Allen et al. 2015). These elaborations strongly suggested that OCNL manipulation not only augmented lipid productivity of *C. subellipsoidea* cells but also produced the most preferable fatty acid profiles for the use of *C. subellipsoidea* as a bio-fuel resource.

The augmented lipid productivity of *C. subellipsoidea* has been demonstrated by OCNL strategy. However, the metabolites related to lipid biosynthesis as well as the interdependence relation of metabolites and lipids under OCNL manipulation needed to be discussed to further expand the biomass utilization of *C. subellipsoidea*. As depicted in

The data were expressed as the mean \pm SD values for three independent biological replicates ($n=3$), which was consistent with the date shown in Table 3. UDP-Glucose, UDP-galactose, G3P, PEP, OAA, and α -KG were the abbreviations of uridine diphosphate glucose, uridine diphosphate galactose, glyceraldehyde-3-phosphate, phosphoenolpyruvate, oxaloacetate, and α -ketoglutarate, respectively

Fig. 3, glycolysis is the metabolic pathway that converts glucose into pyruvate with the generation of energy molecules (i.e. ATP or NADH). In this study, sucrose, UDP-galactose, and UDP-glucose metabolites were detected in OCNL-treated *C. subellipsoidea* cells (Table 3). The continual reduction of three metabolites indicated that glycolysis activities might be significantly strengthened since these metabolites could be converted to glucose and the accumulated glucose could be integrated into glycolysis. In particular, sucrose significantly decreased from 40.29 mg/g to 21.55 mg/g across 72 h of OCNL treatment, which implied that sucrose might be an important contributor for glycolysis and had crucial effect on the lipids biosynthesis of *C. subellipsoidea* (Fig. 2; Table 3). This finding was inconsistent with the report of Lv et al. (2016), where elevated

level of sucrose was detected when *H. pluvialis* cells synthesized astaxanthin. Such discrepancy might be due to different microalga species with different target products (astaxanthin in *H. pluvialis*; lipids in *C. subellipsoidea*) to result two alga species perform different metabolic behavior. Some other metabolites also provided significant entry points into glycolysis pathway. As shown in Table 3 and Fig. 3, the down-regulations of lactate and alanine indicated that the two metabolites were effectively converted to pyruvate intermediate in glycolysis. Meanwhile, one choline and three choline-containing metabolites (i.e. trimethylamine, phosphocholine and sn-Glycero-3-p) were also detected in OCNL-treated cells. The continual decrease of phosphocholine from 0.15 to 0.01 mg/g demonstrated that this choline-containing metabolite was effectively converted to choline molecule. While accumulated choline had two branches: one is into trimethylamine and the other into sn-Glycero-3-p. The relatively constant of trimethylamine (from 0.0041 to 0.0039 mg/g) suggested that most of choline might be integrated into sn-Glycero-3-p branch, which could be seen from the increased concentration 0.07 to 0.42 mg/g (approximate 6.0-fold). Sn-Glycero-3-p could be further used to synthesize G-3-P intermediate in glycolysis. In light of conversion between choline and choline-containing metabolites, sn-Glycero-3-p might be as an important contributor for glycolysis pathway (Figs. 2, 3). Interestingly, the precursors of most detected amino acids are exactly the intermediates of glycolysis (Fig. 3). For instance, the precursor of serine, threonine, and glycine was G3P; PEP was the precursor of phenylalanine as well as pyruvate was the precursor of tyrosine and lysine; ethanolamine and alanine could also be interconverted into pyruvate. However, most of the amino acids associated with intermediates of glycolysis showed continual decrease under OCNL treatment. Lee et al. (2014) once reported that N-starvation usually lead to a reduction of *de novo* amino acid biosynthesis and increment in fatty acids content. Therefore, the decreased levels of amino acids in this study might contribute to the accumulation of lipids. In addition, the down-regulated ethanolamine metabolite (from 1.90 to 0.493 mg/g) was also detected in OCNL-treated *C. subellipsoidea* cells, which also supported pyruvate accumulation and then strengthened glycolysis (Fig. 3).

Pyruvate was further converted into acetyl-CoA, which was an important pivot for TCA cycle and other biochemical activities. However, some intermediates such as malate, α -KG, succinate, and fumarate existed in TCA cycle showed significant reduction in OCNL-treated cells (Table 3; Fig. 3). Therefore, it could be inferred that TCA cycle was down-regulated to enable more acetyl-CoA from pyruvate or acetate into fatty acids pathway (Fig. 3). On the other hand, some detected amino acid metabolites could be synthesized by intermediates in TCA cycle. For instance,

asparagine could be synthesized by oxaloacetic acid (OAA) as well as α -ketoglutarate was used for glutamate and proline synthesis (Fig. 3). Obviously, *C. subellipsoidea* cells treated with OCNL demonstrated a unique amino acid metabolic profile that asparagine was synthesized in lower amounts while glutamate and proline showed a high accumulation. Lv et al. (2016) reported that proline and glutamic acid were common cytoprotective metabolites and played important roles in enhancing the stability of cell membrane. Therefore, the up-regulations of proline (0.14 to 0.53 mg/g) and glutamic acid (7.47 to 9.11 mg/g) indicated that the two amino acids might be important regulatory factors to protect *C. subellipsoidea* cells from nutrition-limitation stress. In addition, OCNL-treated cells produced lower amounts of formate and aminobutyrate metabolites, which could be converted into fumarate and succinate intermediates in TCA cycle (Table 3; Fig. 3). However, the slight accumulation of the two intermediates was generally negligible for promoting TCA cycle.

Collectively, the down-regulations of TCA and amino acid metabolites response to OCNL manipulation might promote most part of energy and acetyl-CoA toward fatty acids pathway. As shown in Fig. 3 and Table 2, acetyl-CoA flowed into fatty acid pathway to mainly synthesize palmitic acid (C16:0), stearic acid (C18:0), oleic acid (C18:1), hexadecadienoic acid (C16:2), hexadecatrienoic acid (C16:3), linoleic acid (C18:2), and linolenic acid (C18:3). It could be also seen from the attached list data in Table 2 that C16 fatty acids (i.e. C16:0, C16:2, and C16:3) showed successional reduction as well as all C18 fatty acids (i.e. C18:0, C18:1, C18:2, and C18:3) firstly increased and then decreased at different extent with the cultivation duration from 144 to 216 h. Although precise carbon partitioning (i.e. acetyl-CoA) into individual fatty acid was still not well understood, these results indicated that the reduction of C16 fatty acids might be mostly used for C18 fatty acids biosynthesis, especially C18:1 was increased from 24.28 to 42.13%. Moreover, C18:2 and C18:3 showed increment from 10.54 to 17.06% and 16.48 to 27.32%, respectively. Lamers et al. (2012) reported that oleic acid (C18:1) was the main constituent in the formation of lipid bodies in microalgae cells. Therefore, it could be inferred that the accumulation of C18:1 caused more lipid bodies in OCNL-treated *C. subellipsoidea* cells in this study (data not shown).

Conclusion

A preferred OCNL strategy for augmenting lipid productivity of *C. subellipsoidea* has been demonstrated. The findings not only promoted the potential of emerging oleaginous model alga *C. subellipsoidea* for biofuels production,

but also might be available in other microalgae culture systems for lipids resource by nitrogen manipulation. Further, most part of energy and metabolic flux (e.g. acetyl-CoA) derived from TCA cycle and glycolysis flowed into fatty acids pathway to strengthen the proportions of saturated and monounsaturated fatty acids response to OCNL manipulation. Although precise carbon partitioning among individual fatty acid was still not well understood, the information obtained in this study would pave the way for promulgating biosynthesis of algal lipids.

Acknowledgements This work was supported by National Natural Science Foundation of China (21676228) and Scientific Research Fund of Hunan Provincial Education Department (16B254), Hunan Provincial Natural Science Foundation of China (2017JJ3300), and Collaborative Innovation Center of New Chemical Technologies for Environmental Benignity and Efficient Resource Utilization.

References

- Allen JW, DiRusso CC, Black PN (2015) Triacylglycerol synthesis during nitrogen stress involves the prokaryotic lipid synthesis pathway and acyl chain remodeling in the microalgae *Coccomyxa subellipsoidea*. *Algal Res* 10:110–120
- Arumugam M, Agarwal A, Arya MC, Ahmed Z (2013) Influence of nitrogen sources on biomass productivity of microalgae *Scenedesmus bijugatus*. *Bioresour Technol* 131:246–249
- Benavente-Valdés JR, Aguilar C, Contreras-Esquivel JC, Méndez-Zavala A, Montañez J (2016) Strategies to enhance the production of photosynthetic pigments and lipids in *Chlorophyceae* species. *Biotechnol Rep* 10:117–125
- Blanc G, Agarkova I, Grimwood J, Kuo A, Brueggeman A, Duniagan DD, Gurnon J, Ladunga I, Lindquist E, Lucas S, Pangilinan J, Pröschold T, Salamov A, Schmutz J, Weeks D, Yamada T, Lomsadze A, Borodovsky M, Claverie JM, Grigoriev IV, Van Etten JL (2012) The genome of the polar eukaryotic microalga *Coccomyxa subellipsoidea* reveals traits of cold adaptation. *Genome Biol* 13:R39
- Chen CY, Yeh KL, Aisyah R, Lee DJ, Chang JS (2011) Cultivation, photobioreactor design and harvesting of microalgae for biodiesel production: a critical review. *Bioresour Technol* 102:71–81
- Coruzzi G, Bush DR (2001) Nitrogen and carbon nutrient and metabolite signaling in plants. *Plant Physiol* 125:61–64
- Guccione A, Biondi N, Sampietro G, Rodolfi L, Bassi N, Tredici MR (2014) *Chlorella* for protein and biofuels: from strain selection to outdoor cultivation in a Green Wall Panel photobioreactor. *Biotechnol Biofuels* 7:1–12
- Han FF, Huang JK, Li YG, Wang WL, Wan MX, Shen GM, Wang J (2013) Enhanced lipid productivity of *Chlorella pyrenoidosa* through the culture strategy of semi-continuous cultivation with nitrogen limitation and pH control by CO₂. *Bioresour Technol* 136:418–424
- Hultberg M, Jönsson HL, Bergstrand KJ, Carlsson AS (2014) Impact of light quality on biomass production and fatty acid content in the microalga *Chlorella vulgaris*. *Bioresour Technol* 159:465–467
- Klok AJ, Lamers PP, Martens DE, Draaisma RB, Wijffels RH (2014) Edible oils from microalgae: insights in TAG accumulation. *Trends Biotechnol* 32:521–528
- Knothe G (2014) A comprehensive evaluation of the cetane numbers of fatty acid methyl esters. *Fuel* 119:6–13
- Kováčik J, Klejduš B, Babula P, Hedbavny J (2015) Nitric oxide donor modulates cadmium-induced physiological and metabolic changes in the green alga *Coccomyxa subellipsoidea*. *Algal Res* 8:45–52
- Lamers PP, Janssen M, De Vos RCH, Bino RJ, Wijffels RH (2012) Carotenoid and fatty acid metabolism in nitrogen starved *Dunaliella salina*, a unicellular green microalga. *J Biotechnol* 162:21–27
- Lee SY, Kim SH, Hyun SH, Suh HW, Hong SJ, Cho BK, Lee CG, Lee H, Choi HK (2014) Fatty acids and global metabolites profiling of *Dunaliella tertiolecta* by shifting culture conditions to nitrate deficiency and high light at different growth phases. *Process Biochem* 49:996–1004
- Liu TT, Li YQ, Liu F, Wang C (2016) The enhanced lipid accumulation in oleaginous microalga by the potential continuous nitrogen limitation CNL strategy. *Bioresour Technol* 203:150–159
- Lv HX, Xia F, Liu M, Cu XG, Wahid F, Jia SR (2016) Metabolomic profiling of the astaxanthin accumulation process induced by high light in *Haematococcus pluvialis*. *Algal Res* 20:35–43
- Meng YY, Jiang JP, Wang HT, Cao XP, Xue S, Yang Q, Wang WL (2015) The characteristics of TAG and EPA accumulation in *Nannochloropsis oceanica* IMET1 under different nitrogen supply regimes. *Bioresour Technol* 179:483–489
- Msanje J, Xu D, Konda AR, Casas-Mollano JA, Awada T, Cahoon EB, Cerutti H (2012) Metabolic and gene expression changes triggered by nitrogen deprivation in the photoautotrophically grown microalgae *Chlamydomonas reinhardtii* and *Coccomyxa* sp. C-169. *Phytochemistry* 75:50–59
- Mujtaba G, Choi W, Lee CG, Lee K (2012) Lipid production by *Chlorella vulgaris* after a shift from nutrient-rich to nitrogen starvation conditions. *Bioresour Technol* 123:279–283
- Pancha I, Chokshi K, George B, Ghosh T, Paliwal C, Maurya R, Mishra S (2014) Nitrogen stress triggered biochemical and morphological changes in the microalgae *Scenedesmus* sp. CCNM 1077. *Bioresour Technol* 156:146–154
- Peccia J, Haznedaroglu B, Gutierrez J, Zimmerman JB (2013) Nitrogen supply is an important driver of sustainable microalgae biofuel production. *Trends Biotechnol* 31:134–138
- Praveenkumar R, Shameera K, Mahalakshmi G, Akbarsha MA, Thajuddin N (2012) Influence of nutrient deprivations on lipid accumulation in a dominant indigenous microalga *Chlorella* sp., BUM11008: evaluation for biodiesel production. *Biomass Bioenergy* 37:60–66
- Rios LF, Klein BC, Luz LF Jr, Maciel Filho R, Wolf Maciel MR (2015) Nitrogen starvation for lipid accumulation in the microalga species *Desmodesmus* sp. *Appl Biochem Biotechnol* 175:469–476
- Shi XM, Chen F, Yuan JP, Chen H (1997) Heterotrophic production of lutein by selected *Chlorella* strains. *J Appl Phycol* 9:445–450
- Wan C, Alam MA, Zhao XQ, Zhang XY, Guo SL, Ho SH, Chang JS, Bai FW (2015) Current progress and future prospect of microalgal biomass harvest using various flocculation technologies. *Bioresour Technol* 184:251–257
- Wang X, Shen ZY, Miao XL (2016) Nitrogen and hydrophosphate affects glycolipids composition in microalgae. *Sci Rep*. doi:10.1038/srep30145
- Yao Y, Lu Y, Peng KT, Huang T, Niu YF, Xie WH, Yang WD, Liu JS, Li HY (2014) Glycerol and neutral lipid production in the oleaginous marine diatom *Phaeodactylum tricorutum* promoted by overexpression of glycerol-3-phosphate dehydrogenase. *Biotechnol Biofuels* 7:110